Journal of Zhejiang University SCIENCE A
ISSN 1009-3095
http://www.zju.edu.cn/jzus
E-mail: jzus@zju.edu.cn

Behavior of preloaded RC beams strengthened with CFRP laminates

ZHANG Ai-hui (张爱晖)†, JIN Wei-liang (金伟良), LI Gui-bing (李贵炳)†

(*Department of Civil Engineering, Zhejiang University, Hangzhou 310027, China*)

†E-mail: zah@zju.edu.cn; liguibing@zju.edu.cn

Received May 20, 2005; revision accepted Nov. 11, 2005

Abstract: Eighteen reinforced concrete beams, including 16 beams strengthened with CFRP laminate at different levels of preload and 2 control beams, were tested to investigate the influence of preload level on flexural behavior of CFRP-strengthened RC beam. The experimental parameters include rebar ratios, number of plies of CFRP laminates and preload level at the time of strengthening. Theoretical analysis was also carried out to explain the experimental phenomena and results. The experimental and theoretical results indicated that the preload level has more influence on the stiffness and deflection of the strengthened beam, both at post-cracking and post-yielding stage, than that on the yielding and ultimate flexural strength of the strengthened beam. The main failure mode of CFRP-strengthened beam is the intermediate crack-induced debonding of CFRP laminates, provided that the development length of CFRP laminates and shear capacity of the beam are sufficient.

Key words: Beam, Strengthen, CFRP, Flexural behavior, Preload level
doi:10.1631/jzus.2006.A0436 **Document code:** A **CLC number:** TU375.1

INTRODUCTION

Externally bonded fiber reinforced polymer (FRP) composites can be used to improve the flexural strength of structural members. To evaluate the flexural performance of the strengthened members, it is necessary to study the flexural stiffness of FRP-strengthened RC members at different stages, such as pre-cracking, post-cracking and post-yielding.

Up to now, only very few studies were focused on the structural members strengthened under preloading or pre-cracking (Arduini and Nanni, 1997; Norris *et al*., 1992; Sharif *et al*., 1994; Shin and Lee, 2003). Most of researches did not initiate the actual service state of the existing structural members completely. Actually these structures are always subjected to some applied load and sometimes exhibit flexural cracks.

No codes and standards have consistently taken the influence of preload level into account, because there are not enough experimental data for investigating the influence of the preload level on flexural performance. This paper presents an experimental and analytical investigation to study the influence of preload level on ultimate strength and flexural stiffness of CFRP-strengthened beams, to accumulate basic data for supplementing codes and standards, and to provide reference for engineering application.

EXPERIMENTAL PROGRAM

In this work, 16 CFRP-strengthened RC beams and 2 control beams without strengthening were tested. All beams were 2 500 mm long, and had 150 mm wide, 250 mm high cross sections. Fig.1 shows the dimensions and the reinforcement arrangement of the specimens. These specimens were separated into series A with rebar ratio of 0.84% (two 12 mm diameter rebar) and series B with rebar ratio of 1.52% (two 16 mm diameter rebar). The closed-type stirrups of 8 mm-diameter bars were spaced at either 100 mm or 70 mm along the beam length for series A and B respectively. All beams were designed for flexural

* Project (No. 03HK03) supported by the Science and Technology Development Foundation for College and University of Shanghai, China

failure in order to study the flexural behavior of the strengthened beams.

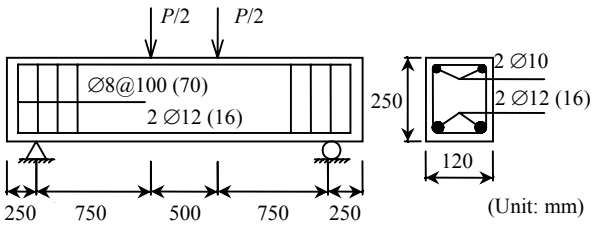

Fig.1 Specimen details and reinforcement arrangement

The parameters considered in this paper are preload level at the time of strengthening, plies of CFRP laminates, and rebar ratio. Specimen details are summarized in Table 1. Specimens are labelled as SPL, where *S*, *P*, and *L* stand for rebar ratio (0.84% for series A and 1.52% for series B), plies of CFRP (*P*=1, 2), and the preload level (*L*=0, 3, 6, and 8, correspond to 0, 30%, 60% and 80% of nominal flexural strength of the control beams respectively). Beam nominal flexural strength is calculated by assuming equivalent concrete compressive stress block as given in the ACI (2002). For series A and B, beams strengthened with one ply of CFRP laminate are termed sub-series A1 and B1, with two plies of CFRP laminates are termed A2 and B2, respectively. The strengthening length of CFRP laminate is determined as 1 800 mm long to avoid premature failure, with width of 120 mm.

Table 1 Specimen and experimental parameters

Specimens		Rebar ratio	CFRP (plies)	Sust. load[1]	Remarks[2]
A	B				
AC	BC	0.84% (1.52%)	0	—	C.B.
A10	B10		1	—	I.S.
A20	B20		2	—	I.S.
A13	B13		1	$0.3P_y$	—
A16	B16		1	$0.6P_y$	—
A18	B18		1	$0.8P_y$	—
A23	B23		2	$0.3P_y$	—
A26	B26		2	$0.6P_y$	—
A28	B28		2	$0.8P_y$	—

[1] P_y: nominal flexural strength of the control beams calculated by ACI 318-02; [2] C.B.: control beam; I.S.: initially strengthened beams

Concrete with cube compressive strength of f_c=23.0 MPa was used. The yielding strength of the rebar was f_y=335 MPa. The properties of CFRP laminate were provided by the manufacturer and had ultimate tensile strength of f_{fu}=3 350 MPa, Young's modulus of E_f=235 GPa, and thickness of 0.111 mm.

Beams were cured indoor for 28 d, the tension face of the beam to bond CFRP laminate was ground to ensure good bonding. Then loads were applied to the desired preload level as shown in Table 1. While maintaining this load, on the clean and flat surface, primer, epoxy, and CFRP laminates were applied in sequence. Infrared heating was used to accelerate the solidification of epoxy resin.

The test beams were simply supported and loaded under four-point bending. Load was applied by oil jack. A safety-holding nut was used in the oil circuit to maintain the preload level during the curing stage. After the epoxy resin had completely cured, additional loads were applied until the failure of the test beam.

Table 2 summarizes the test results and failure modes of all test beams. Fig.2 shows the load-deflection curves of the four sub-series A1, A2, B1 and B2, respectively. Beam AC and BC are the control beams without strengthening. The behavior of the beam presents a typical flexural failure mode, which shows that the loading and testing scheme used in this experiment are correct and reliable.

As shown in Fig.3, two kinds of failure modes occurred on the CFRP-strengthened beams in this experiment. One is the CFRP rupture, another, in the main, is the intermediate flexural-shear crack induced interfacial debonding (Smith and Teng, 2002; Teng *et al*., 2003) (simply as IFC debonding) with the entire depth of concrete cover separation in the constant moment region of the beam. This failure mode of intermediate crack-induced debonding was also reported in literature (Buyukozturk *et al*., 2002; 2004; Oh and Sim, 2004; Sebastian, 2001; Wu and Niu, 2000; Wu and Yin, 2003). Collation of research results revealed that the main failure mode of CFRP-strengthened beam is the intermediate crack-induced debonding of CFRP laminates, provided the development length of CFRP laminates and shear capacity of the strengthened beam are adequate.

The author observed that the IFC debonding process can be separated into an initiation phase and a debonding phase. During the initiation phase, secondary inclined cracks occur at the toe of the critical flexural-shear cracks near the load point. When the

Table 2 Summary of test results

Specimens	Load (kN)			Deflection (mm)			Stiffness (N/mm)		Modes of failure
	P_{cr}	P_y	P_u	δ_{cr}	δ_y	δ_u	B_y	B_u	
AC	9.6	39.6	45.4	0.9	7.5	19.6	4530	480	Flexural failure
A10	9.3	50.4	62.7	0.9	8.4	24.3	5480	774	IFC debonding
A13	10.3	50.0	62.0	1.0	7.5	21.1	6108	882	CFRP rupture
A16	10.3	50.1	63.4	0.9	7.3	23.9	6219	801	IFC debonding
A18	10.0	48.2	63.8	0.8	7.3	24.4	5877	912	IFC debonding
A20	10.0	53.7	75.8	0.9	8.3	27.0	5905	1182	IFC debonding
A23	10.0	54.0	79.8	0.7	7.8	26.2	6197	1402	IFC debonding
A26	10.0	52.7	75.7	0.7	7.3	22.7	6470	1494	IFC debonding
A28	10.0	50.4	73.2	0.7	7.4	21.9	6030	1572	IFC debonding
BC	10.0	65.2	68.7	1.0	7.6	17.2	8400	370	Flexural failure
B10	10.1	76.3	82.4	0.8	9.0	21.0	8073	508	IFC debonding
B13	11.7	80.0	91.3	0.7	7.5	21.0	10044	837	CFRP rupture with concrete crushing
B16	12.1	80.1	92.1	0.7	7.3	23.7	10303	732	CFRP rupture with concrete crushing
B18	12.1	73.6	90.1	0.7	8.4	28.0	7987	842	CFRP rupture with concrete crushing
B20	9.1	74.8	85.1	1.0	9.5	18.8	7729	1108	IFC debonding with Concrete crushing
B23	12.9	84.6	98.6	0.7	7.5	18.6	10544	1261	IFC debonding with concrete crushing
B26	12.6	79.0	95.9	0.8	7.0	18.5	10710	1470	IFC debonding with Concrete crushing
B28	11.5	75.1	93.5	0.8	9.5	21.4	7310	1546	IFC debonding with Concrete crushing

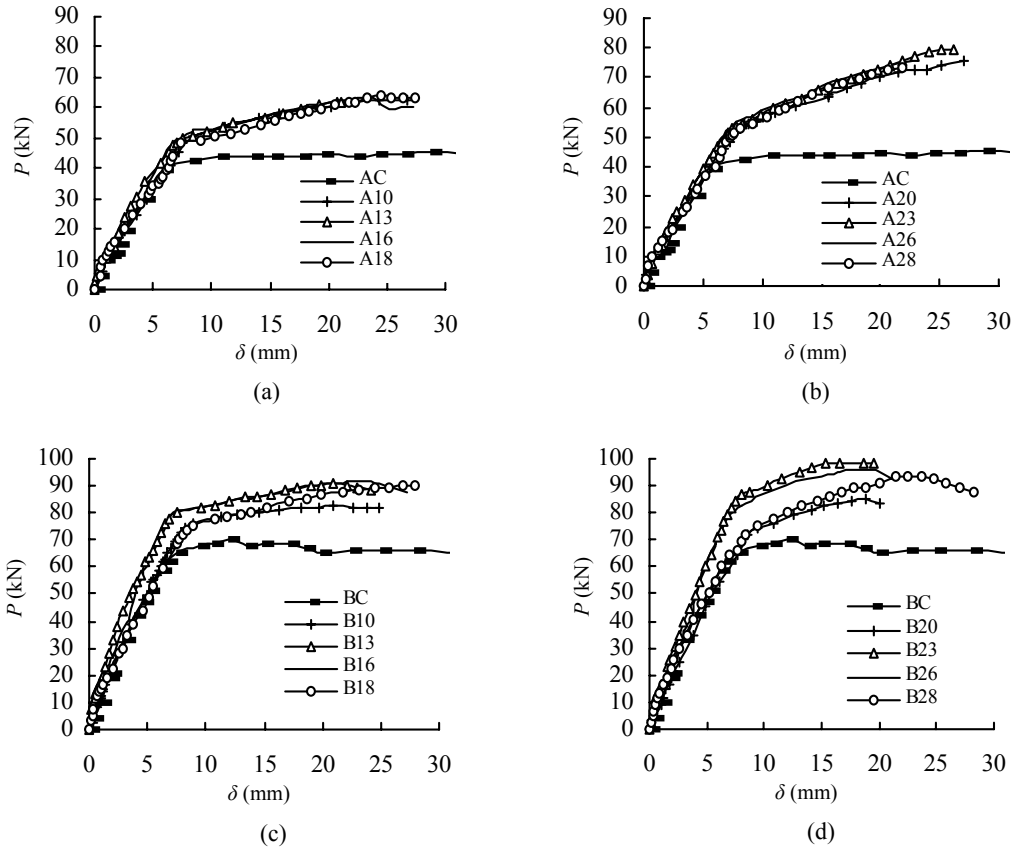

Fig.2 Load-deflection curves. (a) Subseries A1; (b) Subseries A2; (c) Subseries B1; (d) Subseries B2

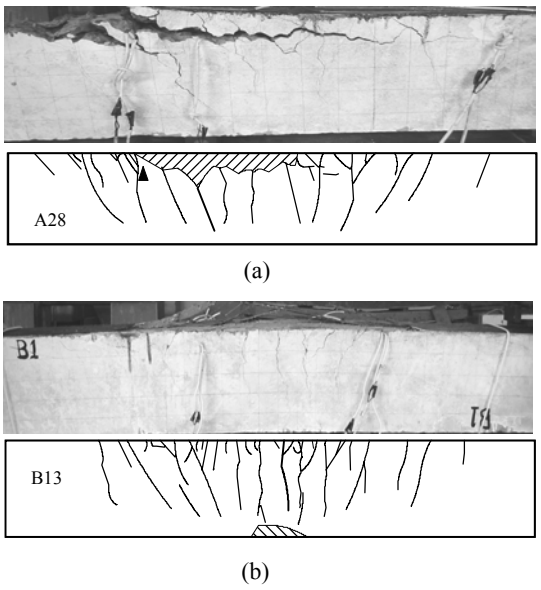

Fig.3 Main failure modes. (a) IFC debonding with concrete cover separation of beam A28; (b) CFRP rupture of beam B13

critical flexural-shear cracks reach a certain width and the interfacial bond-stress exceeds a certain value, a concrete wedge bounded by the flexural-shear and the secondary inclined cracks at the toe of the intermediate flexural-shear crack was formed. The ending of the initiation phase was followed by the process debonding phase when the CFRP debonding length developed toward the end of the laminate. The CFRP debonding region at first increased stably with each subsequent increment of load on the beam. Eventually the CFRP debonding process suddenly runs along the remaining bonded length of CFRP laminates, resulting in complete unzipping of the CFRP laminates from the beam. The energy released by unzipping is sufficient for dislodging the concrete cover wedges off the beam to reveal the flexural rebar.

Beam A10 was initially strengthened with one ply of CFRP laminate. The initial flexural crack load of this beam was almost the same as that of beam AC. However, the crack propagation and the final crack pattern of the beam greatly different from that of beam AC. Beam AC had only a few flexural cracks with much larger width, and beam A10 had much more flexural cracks with smaller width. This indicates that the propagation of cracks was confined by CFRP laminates.

Beam A13 was strengthened with one ply of CFRP laminate, and the preload level was 30% of beam AC's nominal yielding strength. No discernible differences were found in yielding load and ultimate strength between A13 and A10.

Beam A16 was strengthened with one ply of CFRP laminate at the preload level of 60% of nominal strength of beam AC with load-deflection curve following that of beam A10 until the flexural rebar yielding. The ultimate flexural strength increases slightly compared with that of beam A10.

Beam A18 was strengthened at the preload level of 80% of nominal yielding strength of beam AC. Beam A18's load-deflection curve almost follows that of A13 and A16, though the maximum width of the flexural cracks in the constant moment region at the time of strengthening was much larger than that of A13 and A16.

Fig.2b of load-deflection curves of sub-series A2 shows that the influence of preload level on their flexural behavior is similar to that of sub-series A1. The ultimate strength and deflection of any beam strengthened under different preload levels are close to or larger than those of the initially strengthened beam. This indicates that the flexural behavior of the beam strengthened under preload is better than that of the initially strengthened beam AC.

The experimental parameters of series B are the same as those of series A, except that the rebar ratio of the beams is higher than that of series A. However, the failure modes of the beams in series B are different from those of the beams in series A; concrete crushing occurs because the total reinforcements of the beam (including steel reinforcements and CFRP laminates) is close to over-reinforcement. Although concrete crushing occurs at the ultimate stage of almost all the beams, the trend of the influence of preload level on the flexural behavior is similar to that of series A. Within series B, the flexural behavior of the beam strengthened under preload is also better than that of the initially strengthened beam BC.

FLEXURAL STRENGTH ANALYSIS

Histograms of the flexural strengths of all beams are shown in Fig.4. The cracking loads of beams in series A were almost the same except that yielding load and ultimate strength of strengthened beam were

improved due to the reinforcement of CFRP laminates. The ultimate strength of any beam strengthened under different preload levels in each sub-series is close to or slightly higher than that of the initially strengthened one. When the preload level is higher than 30% of nominal yielding strength of the beam, there is only a very little decrease in ultimate strength with the increment of preload.

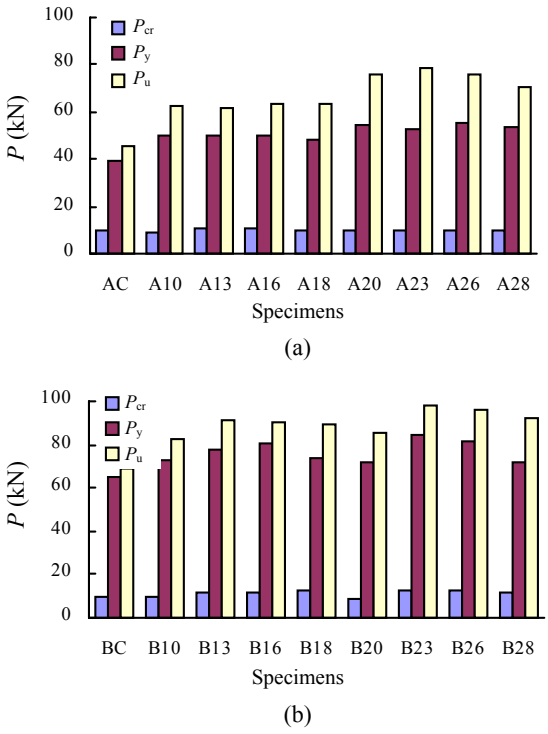

Fig.4 Comparison of cracking, yielding and ultimate loads. (a) Series A; (b) Series B

As shown in Fig.4b, the changing trend of ultimate strength of series B is similar to that of series A, but the increment of ultimate strength is lower than that of its counterpart in series A, because concrete crushing occurred at the ultimate state of the beams.

Theoretical analysis was also carried out in this paper to predict flexural behavior. The theoretical analysis uses the principles of strain compatibility, equilibrium and the constitutive relations of concrete, rebar and composite. The following assumptions were made in the theoretical analysis: (1) Plane sections remain plane; (2) The Rüsch model and the Hognested model were adopted as the constitution law of concrete in compression, as shown in Fig.5; (3) Rebar is assumed to have perfect elasto-plastic response; (4) The unidirectional CFRP laminates are assumed to behave linearly up to failure; (5) No slip between the CFRP laminate and concrete; (6) The concrete is assumed to have no tensile strength.

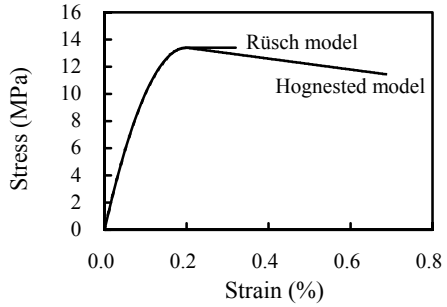

Fig.5 Concrete compression stress-strain relationships

The layered section method is used in the theoretical analysis. The location of the neutral axis x is obtained by solving the following equilibrium equation:

$$\sum_{i=1}^{n}\sigma_{ci}A_{ci}+\sum_{j=1}^{m}\sigma_{sj}A_{sj}+\sigma_{f}A_{f}=0\,, \tag{1}$$

where σ_{ci} is concrete compressive stress of layer i, σ_{sj} steel stress of row j, σ_f stress of CFRP laminates, A_{ci} area of concrete of layer i, A_{sj} area of steel of layer j, A_f area of CFRP laminates, n the total layer number of a layered concrete section, and m total row number of steel rebar.

The nominal moment carrying capacity of a section is obtained by summing the moments of all internal forces about mid-depth of the beam section:

$$M=\sum_{i=1}^{n}\sigma_{ci}A_{ci}(h/2-h_i)+\sum_{j=1}^{m}\sigma_{sj}A_{sj}(h_j-h/2)+\sigma_{f}A_{f}h/2, \tag{2}$$

where h is depth of the section, h_i and h_j are distances between the extreme concrete compressive fiber to the centroid of layer i and j, respectively.

In the calculating, the effect of preload is converted into delay-strain of CFRP laminates which is equal to the concrete strain of the tension face of the beam at the preload level, and then the value of delay-strain, which is obtained from the analysis of the

control beam under the same preload level, is deducted from the strain of the beam's tension face. According to ACI-440, the actual CFRP laminate strain is termed effective strain calculated by

$$\varepsilon_{\mathrm{fe}} = \varepsilon_{\mathrm{c}}\left(\frac{h-x}{x}\right) - \varepsilon_{\mathrm{bi}}, \tag{3}$$

where $\varepsilon_{\mathrm{bi}}$ is initial concrete strain at the strengthening time, which was calculated by strain compatibility and force equilibrium; $\varepsilon_{\mathrm{fe}}$ effective CFRP laminate strain; ε_{c} the beam's tension-face strain; h section depth of specimen; x compressive depth of the section.

The curvature of the section is calculated by

$$\phi = \frac{\varepsilon_{\mathrm{ct}} + \varepsilon_{\mathrm{f}}}{h - h/(2n)}, \tag{4}$$

where $\varepsilon_{\mathrm{ct}}$ is top layer concrete compressive strain; ε_{f} CFRP laminates strain.

Table 3 shows the comparison of CFRP-strains at ultimate strength between the analytical and experimental results. It can be observed that when the Rüsch model is adopted, the analytical results of CFRP-strains accorded well with the experimental responses for series A, whereas there are great disagreements between the analytical and experimental results due to concrete crushing for series B. However when the Hognested model is adopted, the analytical results for series A and B agreed well with the experimental responses.

Table 4 shows the analytical and experimental results of ultimate strength and their statistical results.

As a whole, for series A, regardless of whether the Rüsch model or the Hognested model is adopted, the analytical results accorded well with the experimental responses, with average ratio of analytical to experimental strength being 0.94~0.99, and coefficient of variation being 0.03~0.04. However, for series B, when the Rüsch model is adopted, the average decreases down to 0.82~0.84, with coefficients of variation 0.04. But, if the Hognested model was adopted for series B, the analytical results agreed much better with the experimental responses, with the average of up to 0.92 and coefficient of variation 0.04~0.05.

Table 4 shows the analytical and experimental results of ultimate strength and their statistical results. No discernible difference of analytical ultimate strength was found between considering and not considering the CFRP-strain delay. Therefore, in this paper, the CFRP-strain delay, that is, the effect of preload level can be ignored in calculating ultimate strength of strengthened beam.

INVESTIGATION ON STIFFNESS

As mentioned before, a typical load-deflection curve for a CFRP-strengthened RC beam can be separated into three stages as illustrated in Fig.2. The three stages can be summarized as: (1) Pre-cracking stage ($P<P_{\mathrm{cr}}$); (2) Cracking stage ($P_{\mathrm{cr}}\leq P<P_{\mathrm{y}}$); and (3) Post-yielding stage ($P_{\mathrm{y}}\leq P<P_{\mathrm{u}}$). Where, P_{cr}, P_{y}, P_{u} and

Table 3 FRP-strains at ultimate strength (Unit: με)

Specimens	Experiment	Analysis		Specimens	Experiment	Analysis	
		Rüsch	Hognested			Rüsch	Hognested
A10	10000	11137 (1.11)[a]	12303 (1.23)	B10	8659	4536 (0.52)	8963 (1.04)
A13	11129	10746 (0.97)	11174 (1.00)	B13	10195	4865 (0.48)	8519 (0.84)
A16	9978	10487 (1.05)	10389 (1.04)	B16	10024	4743 (0.47)	8326 (0.83)
A18	9460	8359 (0.88)	9373 (0.99)	B18	6964	3933 (0.56)	7207 (1.03)
A20	10994	10932 (0.99)	11608 (1.06)	B20	10354	4969 (0.48)	8667 (0.84)
A23	9863	8115 (0.82)	8788 (0.89)	B23	6279	4225 (0.67)	6966 (1.11)
A26	7864	7912 (1.01)	8386 (1.07)	B26	6840	4078 (0.60)	6778 (0.99)
A28	7108	7583 (1.07)	7714 (1.09)	B28	6662	3896 (0.58)	6515 (0.98)
Mean		0.99	1.05	Mean		0.55	0.96
COV.		0.10	0.09	COV.		0.13	0.11

[a]Ratio: the number in bracket is the ratio of analytical to experimental results

Table 4 Summary on experimental and analytical results of ultimate strength and statistical data (Unit: kN·m)

Specimens	Experiment	Analysis			
		Rüsch		Hognested	
		CISL[1]	NCISL[2]	CISL[1]	NCISL[2]
A10	23.33	22.65 (0.97)[3]	22.65 (0.97)	23.75 (1.02)	23.75 (1.02)
A20	23.21	22.89 (0.99)	22.65 (0.98)	23.68 (1.02)	23.75 (1.02)
A13	23.78	22.99 (0.97)	22.65 (0.95)	23.74 (1.00)	23.75 (1.00)
A16	23.81	23.33 (0.98)	22.65 (0.95)	23.76 (1.00)	23.75 (1.00)
A18	28.43	25.98 (0.91)	25.98 (0.91)	27.64 (0.97)	27.64 (0.97)
A23	29.93	26.39 (0.88)	25.98 (0.87)	27.63 (0.92)	27.64 (0.92)
A26	28.39	26.77 (0.94)	25.98 (0.92)	27.79 (0.98)	27.64 (0.97)
A28	27.45	27.36 (1.00)	25.98 (0.95)	27.96 (1.02)	27.64 (1.01)
Mean		0.95	0.94	0.99	0.99
COV.		0.04	0.04	0.03	0.03
B10	30.90	26.67 (0.86)	26.67 (0.86)	29.17 (0.94)	29.17 (0.94)
B20	34.24	27.60 (0.81)	27.36 (0.80)	29.95 (0.87)	30.15 (0.88)
B13	34.54	27.84 (0.81)	27.36 (0.79)	30.16 (0.87)	30.15 (0.87)
B16	33.79	28.17 (0.83)	27.36 (0.81)	30.44 (0.90)	30.15 (0.89)
B18	31.91	28.21 (0.88)	28.21 (0.88)	31.57 (0.99)	31.57 (0.99)
B23	36.94	29.52 (0.80)	29.12 (0.79)	32.68 (0.88)	32.89 (0.89)
B26	36.04	29.94 (0.83)	29.12 (0.81)	33.03 (0.92)	32.89 (0.91)
B28	34.65	30.05 (0.87)	29.12 (0.84)	33.48 (0.97)	32.89 (0.95)
Mean		0.84	0.82	0.92	0.92
COV.		0.04	0.04	0.05	0.04
Mean (Total)		0.90	0.89	0.95	0.95
COV. (Total)		0.07	0.07	0.05	0.05

[1]CISL: considering influence of preload level; [2]NCISL: not considering influence of preload level at strengthening; [3]Ratio: the number in bracket is the ratio of analytical to experimental results

P, are the cracking load, load corresponding to the first yield of rebar, ultimate strength, and applied load, respectively. Fig.6 shows average tangent stiffness of all beams at different stages, which are calculated from the experimental data in Table 2. The experimental results of stiffness are summarized as follows: (1) Pre-cracking stage ($P<P_{cr}$). The stiffness of all beams at this stage is very discrete, because the deflections of all beams are too small under this load level. Therefore, it is useless to discuss their diversities here. (2) Cracking stage ($P_{cr}\leq P<P_y$). The average tangent stiffness of the strengthened beam increases due to the CFRP laminates strengthening. That is to say, the preload level has influence on it, the biggest stiffness of the strengthened beam occurs in the beam strengthened at the preload level of $0.6P_y$. (3) Post-yielding stage ($P_y\leq P<P_u$). As shown in Figs.6c and 6d, CFRP laminate can be employed to greatly improve the stiffness of the beam at this stage. The figures show that the retrofit technique can effectively increase the stiffness and decrease the deflection of strengthened beams.

As mentioned before, the flexural strength and stiffness of beam strengthened at a certain preload level is higher than that of initially strengthened beam. The stiffness of any beam strengthened under preload, both at the post-cracking and post-yielding stage (Fig.6), is higher than that of the initially strengthened beam. And the same phenomena also occurred in (Shin and Lee, 2003)'s experiment. As found in this experiment, during the post-cracking and post-yielding stage, a number of small flexural cracks vertically to the axis of the beam were initiated in the constant moment region due to the effect of the CFRP laminates; when these flexural cracks extended vertically about 20 mm, their propagation diverted nearly horizontally at the level of the flexural rebars, and then tended to connect with each other in the whole constant moment region with increase of applied load. As a result, the concrete cover tended to be separated or heavily damaged. This resulted in the decrease of beam effective section depth at the constant moment region, and led to the decrease of section stiffness. The earlier the beam was strengthened, the earlier the

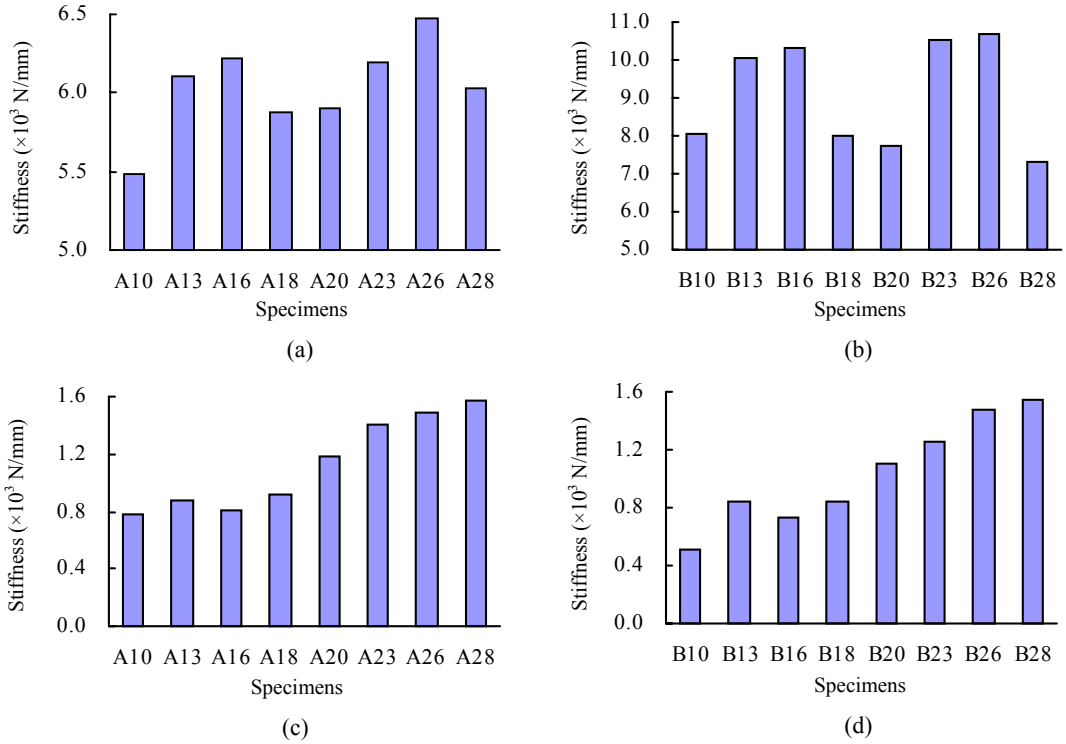

Fig.6 Comparison of average tangent stiffness at different stages: (a), (b) for series A and series B at post-cracking stage; and (c), (d) at post-yielding stage respectively

horizontal cracks were initiated. This indicated that the CFRP laminate of initially strengthened beam performed its function earlier with the applied load, and damaged the concrete cover earlier which could be why the flexural strength and stiffness of the initially strengthened beam was the worst among all the strengthened beams.

However, it would be difficult to clearly discuss the causative reason for the phenomena which is against common sense according to this experiment. To investigate in depth the mechanism of these phenomena, it is necessary to do more experimental and analytical research.

CONCLUSION

The experimental results and analytical investigation in this work led to the conclusions below:

1. The flexural strength of CFRP-strengthened beam is remarkably increased, but the increment of flexural strength is not increase linearly with that of CFRP laminates due to concrete cover separation and concrete crushing.

2. The stiffness of CFRP-strengthened beams is remarkably increased over that of the control beam. That is to say, CFRP laminate performs increases the stiffness and decreases the deflection of structural members subjected to bending.

3. In this work, the preload level, that is, the width of flexural cracks at the time of strengthening had very little influence on the yielding load and ultimate strength of beams strengthened with the same number of CFRP laminates, so it is suggested it can be ignored during calculation of ultimate strength.

4. In this work, the average tangent stiffness of all beams strengthened at a certain preload level, during post-cracking and post-yielding stage, was higher than that of the initially strengthened beams.

5. With sufficient development length of CFRP laminates and shear capacity, the main failure mode of CFRP-strengthened beam is the intermediate crack-induced debonding of CFRP laminates.

References

ACI (ACI-Committee 318), 2002. Building Code Require-

ments for Structural Concrete (ACI 318-02) and Commentary (ACI 318R-02). American Concrete Institute, Farmington Hills, Michigan.

Arduini, M., Nanni, A., 1997. Behavior of precracked RC beams strengthened with carbon FRP sheets. *Journal of Composites for Construction*, **1**(2):63-70. [doi:10.1061/(ASCE)1090-0268(1997)1:2(63)]

Buyukozturk, O., Gunes, O., Karaca, E., 2002. Characterization and Modeling of Debonding in RC Beams Strengthened with FRP Composites. 15th ASCE Engineering Mechanics Conference, Columbia University, New York, p.1-8.

Buyukozturk, O., Gunes, O., Karaca, E., 2004. Progress on understanding debonding problems in reinforced concrete and steel members strengthened using FRP composites. *Construction and Building Materials*, **18**(1):9-19. [doi:10.1016/S0950-0618(03)00094-1]

Norris, T., Saadatmanesh, H., Ehsani, M.R., 1992. Shear and flexural strengthening of R/C beams with carbon fiber sheets. *Journal of Structural Engineering*, **123**(7):903-911. [doi:10.1061/(ASCE)0733-9445(1997)123:7(903)]

Oh, H.S., Sim, J., 2004. Interface debonding failure in beams strengthened with externally bonded GFRP. *Composite Interfaces*, **11**(1):25-42. [doi:10.1163/15685540432268 1037]

Sebastian, W.M., 2001. Significance of midspan debonding failure in FRP-plated concrete beams. *Journal of Structural Engineering*, **127**(7):792-798. [doi:10.1061/(ASCE)0733-9445(2001)127:7(792)]

Sharif, A., AI-Sulaimani, G.J., Basunbul, I.A., Baluch, M.H., Ghaleb, B.N., 1994. Strengthening of initially loaded RC beams using FRP plates. *ACI Structural Journal*, **91**(2):160-168.

Shin, Y.S., Lee, C., 2003. Flexural behavior of RC beams strengthened with carbon fiber-reinforced polymer laminates at different levels of sustaining load. *ACI Structural Journal*, **100**(2):231-239.

Smith, S.T., Teng, J.G., 2002. FRP-strengthened RC beams. I: review of debonding strength models. *Engineering Structures*, **24**(4):385-395. [doi:10.1016/S0141-0296(01)00105-5]

Teng, J.G., Smith, S.T., Yao, J., Chen, J.F., 2003. Intermediate crack-induced debonding in RC beams and slabs. *Construction and Building Materials*, **17**(6-7):447-462. [doi:10.1016/S0950-0618(03)00043-6]

Wu, Z.S., Niu, H., 2000. Study on debonding failure load of RC beams strengthened with FRP sheets. *Journal of Structural Engineering*, **46A**:1431-1441.

Wu, Z.S., Yin, J., 2003. Fracturing behaviors of FRP-strengthened concrete structures. *Engineering Fracture Mechanics*, **70**(10):1339-1355. [doi:10.1016/S0013-7944(02)00100-5]